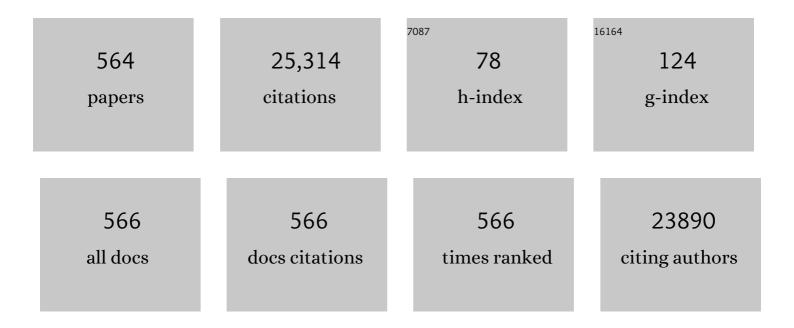
Sridhar Komarneni

List of Publications by Year in descending order

Source: https://exaly.com/author-pdf/1965337/publications.pdf Version: 2024-02-01



#	Article	IF	CITATIONS
1	Fly ash-based geopolymer: clean production, properties and applications. Journal of Cleaner Production, 2016, 125, 253-267.	4.6	629
2	Feature article. Nanocomposites. Journal of Materials Chemistry, 1992, 2, 1219.	6.7	497
3	Microwave-hydrothermal synthesis of ceramic powders. Materials Research Bulletin, 1992, 27, 1393-1405.	2.7	480
4	Electronic Structure Tuning in Ni ₃ FeN/r-GO Aerogel toward Bifunctional Electrocatalyst for Overall Water Splitting. ACS Nano, 2018, 12, 245-253.	7.3	462
5	Synthesis, properties and applications of ZnO nanomaterials with oxygen vacancies: A review. Ceramics International, 2018, 44, 7357-7377.	2.3	369
6	Oxygen defects-mediated Z-scheme charge separation in g-C3N4/ZnO photocatalysts for enhanced visible-light degradation of 4-chlorophenol and hydrogen evolution. Applied Catalysis B: Environmental, 2017, 206, 406-416.	10.8	333
7	Microwaveâ^Polyol Process for Pt and Ag Nanoparticles. Langmuir, 2002, 18, 5959-5962.	1.6	321
8	Synthesis of Smectite Clay Minerals: A Critical Review. Clays and Clay Minerals, 1999, 47, 529-554.	0.6	288
9	Direct Synthesis of Titanium-Substituted Mesoporous SBA-15 Molecular Sieve under Microwaveâ ^{~•} Hydrothermal Conditions. Chemistry of Materials, 2001, 13, 552-557.	3.2	262
10	Biomolecule-Assisted Synthesis of Highly Ordered Snowflakelike Structures of Bismuth Sulfide Nanorods. Journal of the American Chemical Society, 2004, 126, 54-55.	6.6	258
11	Catalytic fast pyrolysis of biomass with mesoporous ZSM-5 zeolites prepared by desilication with NaOH solutions. Applied Catalysis A: General, 2014, 470, 115-122.	2.2	252
12	Ordered SBA-15 Nanorod Arrays Inside a Porous Alumina Membrane. Journal of the American Chemical Society, 2004, 126, 8650-8651.	6.6	246
13	Microwaveâ€Hydrothermal Synthesis of Nanophase Ferrites. Journal of the American Ceramic Society, 1998, 81, 3041-3043.	1.9	244
14	Defect-rich ZnO nanosheets of high surface area as an efficient visible-light photocatalyst. Applied Catalysis B: Environmental, 2016, 192, 8-16.	10.8	231
15	Confined Formation of Ultrathin ZnO Nanorods/Reduced Graphene Oxide Mesoporous Nanocomposites for High-Performance Room-Temperature NO ₂ Sensors. ACS Applied Materials & Interfaces, 2016, 8, 35454-35463.	4.0	210
16	Capture of Radioactive Cesium and Iodide Ions from Water by Using Titanate Nanofibers and Nanotubes. Angewandte Chemie - International Edition, 2011, 50, 10594-10598.	7.2	208
17	Electro-peroxone treatment of Orange II dye wastewater. Water Research, 2013, 47, 6234-6243.	5.3	182
18	Highly stable supercapacitors with MOF-derived Co ₉ S ₈ /carbon electrodes for high rate electrochemical energy storage. Journal of Materials Chemistry A, 2017, 5, 12453-12461.	5.2	180

#	Article	IF	CITATIONS
19	Microwave-hydrothermal processing for synthesis of electroceramic powders. Journal of Materials Research, 1993, 8, 3176-3183.	1.2	179
20	Amine-modified mesocellular silica foams for CO2 capture. Chemical Engineering Journal, 2011, 168, 918-924.	6.6	170
21	Improving the aromatic production in catalytic fast pyrolysis of cellulose by co-feeding low-density polyethylene. Applied Catalysis A: General, 2013, 455, 114-121.	2.2	168
22	Microwave–Hydrothermal Crystallization of Polymorphic MnO ₂ for Electrochemical Energy Storage. Journal of Physical Chemistry C, 2013, 117, 10770-10779.	1.5	168
23	Room-temperature gas sensors based on ZnO nanorod/Au hybrids: Visible-light-modulated dual selectivity to NO2 and NH3. Journal of Hazardous Materials, 2020, 381, 120919.	6.5	168
24	Synthesis and deposition of ultrafine Pt nanoparticles within high aspect ratio TiO2 nanotube arrays: application to the photocatalytic reduction of carbon dioxide. Journal of Materials Chemistry, 2011, 21, 13429.	6.7	152
25	Porous carbons prepared by direct carbonization of MOFs for supercapacitors. Applied Surface Science, 2014, 308, 306-310.	3.1	151
26	Hydrothermal Preparation of Ultrafine Ferrites and Their Sintering. Journal of the American Ceramic Society, 1988, 71, C-26-C-28.	1.9	148
27	Microwave-hydrothermal processing of titanium dioxide. Materials Chemistry and Physics, 1999, 61, 50-54.	2.0	148
28	Microwave-Hydrothermal Synthesis and Characterization of Zirconium Substituted SBA-15 Mesoporous Silica. Journal of Physical Chemistry B, 2001, 105, 8356-8360.	1.2	144
29	Bulk synthesis and selective exchange of strontium ions in Na4Mg6Al4Si4O20F4 mica. Nature, 1992, 357, 571-573.	13.7	139
30	Nanocomposites of hierarchical ultrathin MnO2 nanosheets/hollow carbon nanofibers for high-performance asymmetric supercapacitors. Applied Surface Science, 2019, 463, 931-938.	3.1	137
31	Control over Microporosity of Ordered Microporousâ^'Mesoporous Silica SBA-15 Framework under Microwave-Hydrothermal Conditions:Â Effect of Salt Addition. Chemistry of Materials, 2001, 13, 4573-4579.	3.2	133
32	Rational design of self-supported Cu@WC core-shell mesoporous nanowires for pH-universal hydrogen evolution reaction. Applied Catalysis B: Environmental, 2021, 280, 119451.	10.8	133
33	Microwave-Assisted Polyol Process for Synthesis of Ni Nanoparticles. Journal of the American Ceramic Society, 2006, 89, 1510-1517.	1.9	132
34	Reactions of Cu2+ and Pb2+ with Mg/Al layered double hydroxide. Applied Clay Science, 2007, 37, 143-148.	2.6	129
35	Biomolecule-Assisted Reduction in the Synthesis of Single-Crystalline Tellurium Nanowires. Advanced Materials, 2004, 16, 1629-1632.	11.1	128
36	Synthesis of ZnO with and without microwaves. Materials Research Bulletin, 2000, 35, 1843-1847.	2.7	126

#	Article	IF	CITATIONS
37	Cr(VI) reduction and immobilization by novel carbonaceous modified magnetic Fe3O4/halloysite nanohybrid. Journal of Hazardous Materials, 2016, 309, 151-156.	6.5	126
38	Electrodeposition preparation of NiCo2O4 mesoporous film on ultrafine nickel wire for flexible asymmetric supercapacitors. Chemical Engineering Journal, 2018, 345, 31-38.	6.6	126
39	Visible light photocatalytic activity enhancement of Ag 3 PO 4 dispersed on exfoliated bentonite for degradation of rhodamine B. Applied Catalysis B: Environmental, 2016, 182, 26-32.	10.8	124
40	Extremely enhanced CO2 uptake by HKUST-1 metal–organic framework via a simple chemical treatment. Microporous and Mesoporous Materials, 2014, 183, 69-73.	2.2	122
41	Interface Reaction for the Self-Assembly of Silver Nanocrystals under Microwave-Assisted Solvothermal Conditions. Chemistry of Materials, 2005, 17, 856-860.	3.2	120
42	Polyethylenimine functionalized halloysite nanotubes for efficient removal and fixation of Cr (VI). Microporous and Mesoporous Materials, 2015, 207, 46-52.	2.2	120
43	Microwave-hydrothermal synthesis and characterization of barium titanate powders. Materials Research Bulletin, 2001, 36, 2347-2355.	2.7	119
44	Microwave-hydrothermal processing of metal powders. Journal of Materials Research, 1995, 10, 1687-1692.	1.2	117
45	Novel function for anionic clays: selective transition metal cation uptake by diadochy. Journal of Materials Chemistry, 1998, 8, 1329-1331.	6.7	117
46	A Green Chemical Approach to the Synthesis of Tellurium Nanowires. Langmuir, 2005, 21, 6002-6005.	1.6	117
47	Phosphate removal from solution by composite of MCM-41 silica with rice husk: Kinetic and equilibrium studies. Microporous and Mesoporous Materials, 2016, 224, 51-57.	2.2	115
48	Nanoscale engineering of nitrogen-doped carbon nanofiber aerogels for enhanced lithium ion storage. Journal of Materials Chemistry A, 2017, 5, 8247-8254.	5.2	114
49	Direct Interfacial Growth of MnO ₂ Nanostructure on Hierarchically Porous Carbon for High-Performance Asymmetric Supercapacitors. ACS Sustainable Chemistry and Engineering, 2018, 6, 633-641.	3.2	113
50	Nanophase materials by a novel microwave-hydrothermal process. Pure and Applied Chemistry, 2002, 74, 1537-1543.	0.9	111
51	Microwaveâ€Hydrothermal Synthesis of Monodispersed Nanophase αâ€Fe ₂ O ₃ . Journal of the American Ceramic Society, 2001, 84, 2313-2317.	1.9	111
52	Sol-Gel Fabrication of Epitaxial and Oriented TiO2 Thin Films. Journal of the American Ceramic Society, 1992, 75, 1167-1170.	1.9	108
53	Selective Capture of Iodide from Solutions by Microrosette-like δ-Bi ₂ O ₃ . ACS Applied Materials & Interfaces, 2014, 6, 16082-16090.	4.0	107
54	Hierarchical ZnO Nanosheet-Nanorod Architectures for Fabrication of Poly(3-hexylthiophene)/ZnO Hybrid NO ₂ Sensor. ACS Applied Materials & Interfaces, 2016, 8, 8600-8607.	4.0	106

#	Article	IF	CITATIONS
55	Cr(VI) adsorption by montmorillonite nanocomposites. Applied Clay Science, 2016, 124-125, 111-118.	2.6	106
56	Rapid synthesis of mesoporous SBA-15 molecular sieve by a microwave–hydrothermal process. Chemical Communications, 2000, , 2389-2390.	2.2	104
57	Synthesis and Characterization of Poly(vinylidene fluoride)- <i>g</i> sulfonated Polystyrene Graft Copolymers for Proton Exchange Membrane. Macromolecules, 2008, 41, 9130-9139.	2.2	104
58	Light-activated room-temperature gas sensors based on metal oxide nanostructures: A review on recent advances. Ceramics International, 2021, 47, 7353-7368.	2.3	103
59	Microwave-hydrothermal processing of layered anion exchangers. Journal of Materials Research, 1996, 11, 1866-1869.	1.2	102
60	Mineral mesopore effects on nitrogenous organic matter adsorption. Organic Geochemistry, 2004, 35, 355-375.	0.9	102
61	Superselective clay for radium uptake. Nature, 2001, 410, 771-771.	13.7	100
62	Carbon with ultrahigh capacitance when graphene paper meets K ₃ Fe(CN) ₆ . Nanoscale, 2015, 7, 432-439.	2.8	99
63	Highly selective removal of nitrate and perchlorate by organoclay. Applied Clay Science, 2014, 95, 126-132.	2.6	98
64	Uptake of arsenite by synthetic layered double hydroxides. Water Research, 2009, 43, 3884-3890.	5.3	97
65	Novel hydrothermal electrodeposition to fabricate mesoporous film of Ni0.8Fe0.2 nanosheets for high performance oxygen evolution reaction. Applied Catalysis B: Environmental, 2018, 233, 226-233.	10.8	95
66	Microwave–hydrothermal processing for synthesis of layered and network phosphates. Journal of Materials Chemistry, 1994, 4, 1903-1906.	6.7	94
67	Use of Î ³ -zirconium phosphate for Cs removal from radioactive waste. Nature, 1982, 299, 707-708.	13.7	92
68	Selective Cation Exchange in Substituted Tobermorites. Journal of the American Ceramic Society, 1989, 72, 1668-1674.	1.9	91
69	Role of αâ€Fe ₂ O ₃ Morphology on the Color of Red Pigment for Porcelain. Journal of the American Ceramic Society, 2003, 86, 183-185.	1.9	90
70	Visible-light photocatalytic decolorization of Orange II on Cu2O/ZnO nanocomposites. Ceramics International, 2015, 41, 2050-2056.	2.3	88
71	Synthesis of Glass-like Cordierite from Metal Alkoxides and Characterization by 27Al and 29Si MASNMR. Journal of the American Ceramic Society, 1990, 73, 3663-3669.	1.9	85
72	Barium titanate ceramics prepared from conventional and microwave hydrothermal powders. Materials Letters, 1999, 38, 344-350.	1.3	85

#	Article	IF	CITATIONS
73	ZSM-5 zeolite/porous carbon composite: Conventional- and microwave-hydrothermal synthesis from carbonized rice husk. Microporous and Mesoporous Materials, 2005, 86, 145-151.	2.2	84
74	Microwave-Hydrothermal Processing of BiFeO3 and CsAl2PO6. Journal of the American Ceramic Society, 1996, 79, 1409-1412.	1.9	83
75	Microwave-assisted versus conventional synthesis of zeolite A from metakaolinite. Microporous and Mesoporous Materials, 2008, 115, 527-534.	2.2	83
76	Stepwise functionalization of mesoporous crystalline silica materials. Microporous and Mesoporous Materials, 1998, 25, 75-80.	2.2	82
77	Nanocomposite of halloysite nanotubes/multi-walled carbon nanotubes for methyl parathion electrochemical sensor application. Applied Clay Science, 2021, 200, 105907.	2.6	82
78	Advances in recyclable and superior photocatalytic fibers: Material, construction, application and future perspective. Composites Part B: Engineering, 2021, 205, 108512.	5.9	82
79	Synthetic hydrotalcite-type and hydrocalumite-type layered double hydroxides for arsenate uptake. Applied Clay Science, 2010, 48, 631-637.	2.6	81
80	Nucleation of alpha alumina in boehmite gel. Journal of Materials Research, 1990, 5, 278-285.	1.2	80
81	Time-resolved structural analysis of K- and Ba-exchange reactions with synthetic Na-birnessite using synchrotron X-ray diffraction. American Mineralogist, 2007, 92, 380-387.	0.9	80
82	Self‣upportive Mesoporous Ni/Co/Fe Phosphosulfide Nanorods Derived from Novel Hydrothermal Electrodeposition as a Highly Efficient Electrocatalyst for Overall Water Splitting. Small, 2019, 15, e1905201.	5.2	80
83	Selective Exchange and Fixation of Strontium Ions with Ultrafine Na-4-mica. Langmuir, 2001, 17, 4881-4886.	1.6	79
84	An investigation on the use of electrolytic manganese residue as filler in sulfur concrete. Construction and Building Materials, 2014, 73, 305-310.	3.2	79
85	Adsorption of light hydrocarbons on HMS type mesoporous silica. Microporous and Mesoporous Materials, 2003, 65, 267-276.	2.2	78
86	Cellulose-Directed Growth of Selenium Nanobelts in Solution. Chemistry of Materials, 2006, 18, 159-163.	3.2	77
87	Effects of conventional ozonation and electro-peroxone pretreatment of surface water on disinfection by-product formation during subsequent chlorination. Water Research, 2018, 130, 322-332.	5.3	77
88	Surface Charge of Variable Porosity Al2O3(s) and SiO2(s) Adsorbents. Journal of Porous Materials, 2002, 9, 243-256.	1.3	76
89	CO2 adsorption on Santa Barbara Amorphous-15 (SBA-15) and amine-modified Santa Barbara Amorphous-15 (SBA-15) with and without controlled microporosity. Journal of Colloid and Interface Science, 2013, 390, 217-224.	5.0	74
90	Optimizing the distribution of aromatic products from catalytic fast pyrolysis of cellulose by ZSM-5 modification with boron and co-feeding of low-density polyethylene. Applied Catalysis A: General, 2014, 487, 45-53.	2.2	74

#	Article	IF	CITATIONS
91	Influence of Tetrahedral Layer Charge on the Organization of Interlayer Water and Ions in Synthetic Na-Saturated Smectites. Journal of Physical Chemistry C, 2015, 119, 4158-4172.	1.5	74
92	Sustainable seaweed-based one-dimensional (1D) nanofibers as high-performance electrocatalysts for fuel cells. Journal of Materials Chemistry A, 2015, 3, 14188-14194.	5.2	72
93	Partly nitrogenized nickel oxide hollow spheres with multiple compositions for remarkable electrochemical performance. Chemical Engineering Journal, 2019, 358, 531-539.	6.6	72
94	Adsorption of methylene blue and Orange II pollutants on activated carbon prepared from banana peel. Journal of Porous Materials, 2015, 22, 301-311.	1.3	71
95	One-step synthesis of nanostructured mesoporous ZIF-8/silica composites. Microporous and Mesoporous Materials, 2016, 219, 311-316.	2.2	71
96	Mg doped CuO–Fe2O3 composites activated by persulfate as highly active heterogeneous catalysts for the degradation of organic pollutants. Journal of Alloys and Compounds, 2020, 825, 154036.	2.8	71
97	Cr(VI) uptake by a composite of processed diatomite with MCM-41: Isotherm, kinetic and thermodynamic studies. Microporous and Mesoporous Materials, 2018, 260, 84-92.	2.2	69
98	Fast Synthesis of Cerium Oxide Nanoparticles and Nanorods. Journal of Nanoscience and Nanotechnology, 2006, 6, 3812-3819.	0.9	67
99	Investigation of the synergistic effects for p-nitrophenol mineralization by a combined process of ozonation and electrolysis using a boron-doped diamond anode. Journal of Hazardous Materials, 2014, 280, 644-653.	6.5	67
100	A Cs _x WO ₃ /ZnO nanocomposite as a smart coating for photocatalytic environmental cleanup and heat insulation. Nanoscale, 2015, 7, 17048-17054.	2.8	67
101	TiO2/Sepiolite nanocomposites doped with rare earth ions: Preparation, characterization and visible light photocatalytic activity. Microporous and Mesoporous Materials, 2019, 274, 25-32.	2.2	67
102	Na-4-mica: Cd2+, Ni2+, Co2+, Mn2+ and Zn2+ ion exchange. Journal of Materials Chemistry, 1999, 9, 533-539.	6.7	66
103	Thermally stable phosphorus and nickel modified ZSM-5 zeolites for catalytic co-pyrolysis of biomass and plastics. RSC Advances, 2015, 5, 30485-30494.	1.7	66
104	BiOCl dispersed on NiFe–LDH leads to enhanced photo-degradation of Rhodamine B dye. Applied Clay Science, 2015, 109-110, 76-82.	2.6	66
105	Fluoride removal by ordered and disordered mesoporous aluminas. Microporous and Mesoporous Materials, 2014, 197, 156-163.	2.2	65
106	Separate or Simultaneous Removal of Radioactive Cations and Anions from Water by Layered Sodium Vanadate-Based Sorbents. Chemistry of Materials, 2014, 26, 4788-4795.	3.2	65
107	Sol-gel processing of PbTiO ₃ and Pb(Zr _{0.52} Ti _{0.48})O ₃ fibers. Journal of Materials Research, 1992, 7, 992-996.	1.2	64
108	Nanoclay assisted electrochemical exfoliation of pencil core to high conductive graphene thin-film electrode. Journal of Colloid and Interface Science, 2017, 487, 156-161.	5.0	64

#	Article	IF	CITATIONS
109	Synthesis and Dielectric Properties of Solution Sol-Gel-Derived 0.9Pb(Mg1/3Nb2/3)O3-0.1PbTiO3 Ceramics. Journal of the American Ceramic Society, 1991, 74, 2996-2999.	1.9	63
110	Rapid synthesis of AlPO4-11 and cloverite by microwavehydrothermal processing. Microporous and Mesoporous Materials, 1998, 20, 39-44.	2.2	63
111	Template free ZSM-5 from siliceous rice hull ash with varying C contents. Microporous and Mesoporous Materials, 2006, 93, 134-140.	2.2	63
112	Microwave- and conventional-hydrothermal synthesis of CuS, SnS and ZnS: Optical properties. Ceramics International, 2013, 39, 4757-4763.	2.3	63
113	Fabrication, performance and mechanism of MgO meso-/macroporous nanostructures for simultaneous removal of As(<scp>iii</scp>) and F in a groundwater system. Environmental Science: Nano, 2016, 3, 1416-1424.	2.2	61
114	Substituted Tobermorites: 27Al and 29Si MASNMR, Cation Exchange, and Water Sorption Studies. Journal of the American Ceramic Society, 1991, 74, 274-279.	1.9	60
115	Nanocomposite of exfoliated bentonite/g-C3N4/Ag3PO4 for enhanced visible-light photocatalytic decomposition of Rhodamine B. Chemosphere, 2016, 162, 269-276.	4.2	60
116	One-pot green hydrothermal synthesis of bio-derived nitrogen-doped carbon sheets embedded with zirconia nanoparticles for electrochemical sensing of methyl parathion. Ceramics International, 2020, 46, 19713-19722.	2.3	60
117	Fabrication of AgBr/Ag2CrO4 composites for enhanced visible-light photocatalytic activity. Ceramics International, 2015, 41, 12509-12513.	2.3	59
118	Sepiolite-TiO 2 nanocomposites for photocatalysis: Synthesis by microwave hydrothermal treatment versus calcination. Applied Clay Science, 2017, 146, 246-253.	2.6	59
119	Preparation of La2Zr2O7 by Sol-Gel Route. Journal of the American Ceramic Society, 1991, 74, 422-424.	1.9	58
120	Microwave Versus Conventional-Hydrothermal Synthesis of NaY Zeolite. Journal of Porous Materials, 2001, 8, 5-12.	1.3	58
121	N-doped TiO2/sepiolite nanocomposites with enhanced visible-light catalysis: Role of N precursors. Applied Clay Science, 2018, 166, 9-17.	2.6	58
122	Enhancing adsorption capacity of Egyptian diatomaceous earth by thermo-chemical purification: Methylene blue uptake. Journal of Colloid and Interface Science, 2019, 534, 408-419.	5.0	58
123	Solid-State Epitaxial Effects in Structurally Diphasic Xerogel of Pb(Mg1/3Nb2/3)O3. Journal of the American Ceramic Society, 1990, 73, 1024-1025.	1.9	57
124	Manganese doped magnetic cobalt ferrite nanoparticles for dye degradation via a novel heterogeneous chemical catalysis. Materials Chemistry and Physics, 2020, 240, 122181.	2.0	56
125	Titania gel spheres by a new sol-gel process. Materials Letters, 1985, 3, 165-167.	1.3	55
126	Preparation and densification of forsterite (Mg2SiO4) by nanocomposite sol-gel processing. Materials Letters, 1990, 9, 405-409.	1.3	55

#	Article	IF	CITATIONS
127	Self-generated N-doped anodized stainless steel mesh for an efficient and stable overall water splitting electrocatalyst. Applied Surface Science, 2019, 480, 655-664.	3.1	55
128	Cation exchange properties of a layered manganic acid. Materials Research Bulletin, 1992, 27, 741-751.	2.7	54
129	Microwave―versus Conventionalâ€Hydrothermal Synthesis of Hydroxyapatite Crystals from Gypsum. Journal of the American Ceramic Society, 1999, 82, 2257-2259.	1.9	54
130	Microwave-hydrothermal process for the synthesis of rutile. Materials Research Bulletin, 2005, 40, 2014-2020.	2.7	54
131	Morphological and Kinetic Studies on Hexagonal Tungstates. Chemistry of Materials, 2007, 19, 185-197.	3.2	54
132	Nanoparticles of magnetite anchored onto few-layer graphene: A highly efficient Fenton-like nanocomposite catalyst. Journal of Colloid and Interface Science, 2018, 532, 161-170.	5.0	54
133	Evaluation of Zn–Al–SO4 layered double hydroxide for the removal of arsenite and arsenate from a simulated soil solution: Isotherms and kinetics. Applied Clay Science, 2014, 95, 119-125.	2.6	53
134	Mechanism of Microwave Heating of Zeolite A. Journal of Porous Materials, 2001, 8, 23-35.	1.3	52
135	Protein-assisted synthesis of single-crystal nanowires of bismuth compounds. Chemical Communications, 2005, , 531.	2.2	52
136	Incomplete phase separation strategy to synthesize P/N co-doped porous carbon with interconnected structure for asymmetric supercapacitors with ultra-high power density. Electrochimica Acta, 2019, 298, 717-725.	2.6	52
137	Novel synthesis of layered double hydroxides (LDHs) from zinc hydroxide. Applied Surface Science, 2017, 396, 799-803.	3.1	51
138	Specific Cadmium Sorption in Relation to the Crystal Chemistry of Clay Minerals. Soil Science Society of America Journal, 1988, 52, 49-53.	1.2	50
139	Sol-gel processing of cordierite: Effect of seeding and optimization of heat treatment. Journal of Materials Research, 1990, 5, 1095-1103.	1.2	50
140	Pore structures of fly ashes activated by Ca(OH)2 and CaSO4 · 2H2O. Cement and Concrete Research, 1995, 25, 417-425.	4.6	50
141	Microwave versus conventional preparation of organoclays from natural and synthetic clays. Applied Clay Science, 2006, 31, 134-141.	2.6	50
142	Conventional- vs microwave-hydrothermal synthesis of tin oxide, SnO2 nanoparticles. Ceramics International, 2009, 35, 3375-3379.	2.3	50
143	In situ stabilization of As and Sb with naturally occurring Mn, Al and Fe oxides in a calcareous soil: Bioaccessibility, bioavailability and speciation studies. Journal of Hazardous Materials, 2014, 273, 247-252.	6.5	50
144	Facile synthesis of mesoporous MOF/silica composites. RSC Advances, 2014, 4, 57501-57504.	1.7	50

#	Article	IF	CITATIONS
145	Nanocomposite aerogels: The SiO ₂ –Al ₂ O ₃ system. Journal of Materials Research, 1993, 8, 3163-3167.	1.2	49
146	Highly sensitive detection of gallic acid based on 3D interconnected porous carbon nanotubes/carbon nanosheets modified glassy carbon electrode. Journal of Materials Research and Technology, 2020, 9, 9422-9433.	2.6	49
147	Diphasic ceramic composites via a sol-gel method. Materials Letters, 1984, 2, 245-247.	1.3	48
148	Solid-state epitaxy demonstrated by thermal reactions of structurally diphasic xerogels: The system Al2O3. Journal of Materials Science Letters, 1986, 5, 21-24.	0.5	48
149	Remarkable electrochemical properties of novel LaNi _{0.5} Co _{0.5} O ₃ /0.333Co ₃ O ₄ hollow spheres with a mesoporous shell. Journal of Materials Chemistry A, 2017, 5, 5838-5845.	5.2	48
150	Self-Assembled Ni ₃ S ₂ Nanosheets with Mesoporous Structure Tightly Held on Ni Foam as a Highly Efficient and Long-Term Electrocatalyst for Water Oxidation. ACS Sustainable Chemistry and Engineering, 2019, 7, 5430-5439.	3.2	48
151	Three-dimensional hierarchical porous carbon coupled with chitosan based electrochemical sensor for sensitive determination of niclosamide. Food Chemistry, 2022, 366, 130563.	4.2	48
152	Zeolites for fixation of cesium and strontium from radwastes by thermal and hydrothermal treatments. Nuclear and Chemical Waste Management, 1981, 2, 259-264.	0.2	47
153	Lowering Crystallization Temperatures by Seeding in Structurally Diphasic Al2O3-MgO Xerogels. Journal of the American Ceramic Society, 1985, 68, C-238-C-240.	1.9	47
154	High temperature oxidation of silicon hexaboride ceramics. Materials Research Bulletin, 2001, 36, 1083-1089.	2.7	47
155	Mechanism of zeolite X crystallization from diatomite. Materials Research Bulletin, 2018, 107, 132-138.	2.7	47
156	Copper sulfide as an excellent co-catalyst with K2S2O8 for dye decomposition in advanced oxidation process. Separation and Purification Technology, 2020, 233, 116057.	3.9	47
157	Porous hydroxyapatite monoliths from gypsum waste. Journal of Materials Chemistry, 1998, 8, 2803-2806.	6.7	46
158	Solid-State NMR and Computational Chemistry Study of Mononucleotides Adsorbed to Alumina. Langmuir, 2006, 22, 9281-9286.	1.6	46
159	Solvothermal preparation of TiO2/saponite nanocomposites and photocatalytic activity. Applied Clay Science, 2009, 46, 363-368.	2.6	46
160	Perchlorate uptake by synthetic layered double hydroxides and organo-clay minerals. Applied Clay Science, 2011, 51, 158-164.	2.6	46
161	Wearable Solid-State Supercapacitors Operating at High Working Voltage with a Flexible Nanocomposite Electrode. ACS Applied Materials & Interfaces, 2016, 8, 25905-25914.	4.0	46
162	Equilibrium and kinetic studies for adsorption of iron from aqueous solution by synthetic Na-A zeolites: Statistical modeling and optimization. Microporous and Mesoporous Materials, 2016, 228, 266-274.	2.2	45

#	Article	IF	CITATIONS
163	Toward Aerogel Electrodes of Superior Rate Performance in Supercapacitors through Engineered Hollow Nanoparticles of NiCo ₂ O ₄ . Advanced Science, 2017, 4, 1700345.	5.6	45
164	Ultrasonic-assisted preparation of halloysite nanotubes/zirconia/carbon black nanocomposite for the highly sensitive determination of methyl parathion. Materials Science and Engineering C, 2021, 123, 111982.	3.8	45
165	Pseudomorphism in xonotlite and tobermorite with Co2+ and Ni2+ exchange for Ca2+ at 25°C. Cement and Concrete Research, 1986, 16, 47-58.	4.6	44
166	Synthesis of 11Ã Al-substituted tobermorite from trachyte rock by hydrothermal treatment. Ceramics International, 2010, 36, 203-209.	2.3	44
167	Characterization and cation exchange properties of zeolite synthesized from fly ashes. Journal of Materials Research, 1998, 13, 3-7.	1.2	43
168	Removal of perchlorate by synthetic organosilicas and organoclay: Kinetics and isotherm studies. Applied Clay Science, 2013, 71, 21-26.	2.6	43
169	BiOCl and TiO 2 deposited on exfoliated ZnCr-LDH to enhance visible-light photocatalytic decolorization of Rhodamine B. Ceramics International, 2017, 43, 5751-5758.	2.3	43
170	Preparation of functionalized kaolinite/epoxy resin nanocomposites with enhanced thermal properties. Applied Clay Science, 2017, 148, 103-108.	2.6	43
171	Low-cost and eco-friendly synthesis of octahedral LiMn2O4 cathode material with excellent electrochemical performance. Ceramics International, 2019, 45, 17183-17191.	2.3	43
172	Precise Cation Recognition in Two-Dimensional Nanofluidic Channels of Clay Membranes Imparted from Intrinsic Selectivity of Clays. ACS Nano, 2022, 16, 4930-4939.	7.3	43
173	Sol-gel synthesis of Ln2(Ln = La, Nd)Ti2O7. Journal of Materials Research, 1992, 7, 2859-2863.	1.2	42
174	Sol-Gel Processing of Some Electroceramic Powders. Journal of Sol-Gel Science and Technology, 1999, 15, 263-270.	1.1	42
175	Efficient degradation of rhodamine B by magnetically separable ZnS–ZnFe2O4 composite with the synergistic effect from persulfate. Chemosphere, 2019, 237, 124547.	4.2	42
176	Quaternary (Fe/Ni)(P/S) mesoporous nanorods templated on stainless steel mesh lead to stable oxygen evolution reaction for over two months. Journal of Colloid and Interface Science, 2020, 561, 576-584.	5.0	42
177	Rapid determination of methyl parathion in vegetables using electrochemical sensor fabricated from biomass-derived and β-cyclodextrin functionalized porous carbon spheres. Food Chemistry, 2022, 384, 132643.	4.2	42
178	Alkali metal ion exchange selectivity of Al-substituted tobermorite. Journal of Materials Research, 1989, 4, 698-703.	1.2	41
179	Methoxy-grafted kaolinite preparation by intercalation of methanol: Mechanism of its structural variability. Applied Clay Science, 2017, 137, 241-248.	2.6	41
180	Reduced graphene oxide/MoS2 hybrid films for room-temperature formaldehyde detection. Materials Letters, 2017, 189, 42-45.	1.3	41

#	Article	IF	CITATIONS
181	In situ construction of porous Ni/Co-MOF@Carbon cloth electrode with honeycomb-like structure for high-performance energy storage. Journal of Porous Materials, 2019, 26, 921-929.	1.3	41
182	Cation-Exchange Properties of (Al + Na)-Substituted Synthetic Tobermorites. Clays and Clay Minerals, 1987, 35, 385-390.	0.6	40
183	Grain Size Dependence of High Power Piezoelectric Characteristics in Nb Doped Lead Zirconate Titanate Oxide Ceramics. Japanese Journal of Applied Physics, 2001, 40, 6907-6910.	0.8	40
184	Three-phase nanocomposites of two nanoclays and TiO2: Synthesis, characterization and photacatalytic activities. Applied Catalysis B: Environmental, 2014, 147, 526-533.	10.8	40
185	AgCl and BiOCl composited with NiFe-LDH for enhanced photo-degradation of Rhodamine B. Separation and Purification Technology, 2015, 156, 789-794.	3.9	40
186	Heavy metal removal from aqueous solutions by tobermorites and zeolites. Nuclear and Chemical Waste Management, 1985, 5, 247-250.	0.2	39
187	Lowering the sintering temperature and enhancing densification by epitaxy in structurally diphasic Al2O3 and Al2O3î—,MgO xerogels. Materials Science and Engineering, 1986, 83, 151-159.	0.1	39
188	Selective exchange of divalent transition metal ions in cryptomelane-type manganic acid with tunnel structure. Journal of Materials Research, 1993, 8, 611-616.	1.2	39
189	Synthesis of Na-A and/or Na-X zeolite/porous carbon composites from carbonized rice husk. Journal of Solid State Chemistry, 2009, 182, 1749-1753.	1.4	39
190	Colloidal pseudocapacitor: Nanoscale aggregation of Mn colloids from MnCl2 under alkaline condition. Journal of Power Sources, 2015, 279, 365-371.	4.0	39
191	Beyond theoretical capacity in Cu-based integrated anode: Insight into the structural evolution of CuO. Journal of Power Sources, 2015, 275, 136-143.	4.0	39
192	Co-Mn-Fe complex oxide catalysts from layered double hydroxides for decomposition of methylene blue: Role of Mn. Applied Clay Science, 2018, 152, 230-238.	2.6	39
193	"Structural instability―induced high-performance NiFe layered double hydroxides as oxygen evolution reaction catalysts for pH-near-neutral borate electrolyte: The role of intercalates. Applied Catalysis B: Environmental, 2020, 263, 118343.	10.8	39
194	Synthesis of Na-4-mica from metakaolinite and MgO: characterization and Sr2+ uptake kinetics. Journal of Materials Chemistry, 1998, 8, 205-208.	6.7	38
195	Uptake of cesium and strontium cations by potassium-depleted phlogopite. Applied Clay Science, 2006, 31, 306-313.	2.6	38
196	An <i>in situ</i> anion exchange induced high-performance oxygen evolution reaction catalyst for the pH-near-neutral potassium borate electrolyte. Journal of Materials Chemistry A, 2019, 7, 6995-7005.	5.2	38
197	A novel Fenton-like system of Fe2O3 and NaHSO3 for Orange II degradation. Separation and Purification Technology, 2020, 230, 115866.	3.9	38
198	Cation exchange equilibria of cesium and strontium with K-depleted biotite and muscovite. Applied Clay Science, 2009, 44, 15-20.	2.6	37

#	Article	IF	CITATIONS
199	In situ reduction for synthesis of nano-sized Cu2O particles on MgCuAl-LDH layers for degradation of orange II under visible light. Ceramics International, 2015, 41, 3191-3196.	2.3	37
200	Orthorhombic LiMnO2 nanorods as cathode materials for lithium-ion batteries: Synthesis and electrochemical properties. Ceramics International, 2016, 42, 9319-9322.	2.3	37
201	Silylation of saponite with 3-aminopropyltriethoxysilane. Applied Clay Science, 2016, 132-133, 133-139.	2.6	37
202	Preparation and in vitro study of lipid nanoparticles encapsulating drug loaded montmorillonite for ocular delivery. Applied Clay Science, 2016, 119, 277-283.	2.6	37
203	N-Doped Porous Carbon Self-Generated on Nickel Oxide Nanosheets for Electrocatalytic N ₂ Fixation with a Faradaic Efficiency beyond 30%. ACS Sustainable Chemistry and Engineering, 2019, 7, 18874-18883.	3.2	37
204	Kinetics and mechanism of thiamethoxam abatement by ozonation and ozone-based advanced oxidation processes. Journal of Hazardous Materials, 2020, 390, 122180.	6.5	37
205	Application of Compositionally Diphasic Xerogels for Enhanced Densification: The System Al2O3-SiO2. Journal of the American Ceramic Society, 1986, 69, C-155-C-156.	1.9	36
206	Crystallization and Seeding Effect in BaAl2Si2O8 Gels. Journal of the American Ceramic Society, 1995, 78, 2521-2526.	1.9	36
207	Water adsorption and desorption isotherms of silica and alumina mesoporous molecular sieves. Journal of Porous Materials, 1996, 3, 99-106.	1.3	36
208	Self-Supported Composite of (Ni,Co) ₃ C Mesoporous Nanosheets/N-Doped Carbon as a Flexible Electrocatalyst for pH-Universal Hydrogen Evolution. ACS Sustainable Chemistry and Engineering, 2020, 8, 5287-5295.	3.2	36
209	Visible-light-driven activation of sodium persulfate for accelerating orange II degradation using ZnMn2O4 photocatalyst. Chemosphere, 2021, 278, 130404.	4.2	36
210	An Evaluation Method of Chromatographic Parameters from the Ion-Exchange Isotherm of Al3+â°'Substituted Tobermorite Cation Exchanger. Separation Science and Technology, 1991, 26, 647-659.	1.3	35
211	Sol-Gel Fabrication of Pb(Zr0.52 Ti0.48)O3 Thin Films Using Lead Acetylacetonate as the Lead Source. Journal of the American Ceramic Society, 1993, 76, 1441-1444.	1.9	35
212	Synthesis of NaÂ2Âmica from metakaolin and its cation exchange properties. Journal of Materials Chemistry, 2001, 11, 2072-2077.	6.7	35
213	Microwave–polyol process for metal nanophases. Journal of Physics Condensed Matter, 2004, 16, S1305-S1312.	0.7	35
214	Facile synthesis of orthorhombic LiMnO2 nanorods by in-situ carbothermal reduction: Promising cathode material for Li ion batteries. Ceramics International, 2017, 43, 10585-10589.	2.3	35
215	Cost-effective large-scale synthesis of oxygen-defective ZnO photocatalyst with superior activities under UV and visible light. Ceramics International, 2017, 43, 1870-1879.	2.3	35
216	Biomass as a Template Leads to CdS@Carbon Aerogels for Efficient Photocatalytic Hydrogen Evolution and Stable Photoelectrochemical Cells. ACS Sustainable Chemistry and Engineering, 2018, 6, 14911-14918.	3.2	35

#	Article	IF	CITATIONS
217	Enhanced Densification by Seeding of Sol-Gel-Derived Aluminum Titanate. Journal of the American Ceramic Society, 1992, 75, 1529-1533.	1.9	34
218	Microwave-assisted synthesis of one-dimensional nanostructures. Journal of Materials Research, 2004, 19, 1649-1655.	1.2	34
219	Nafion/Zirconium Phosphate Composite Membranes for PEMFC Operating at up to 120°C and down to 13% RH. Journal of the Electrochemical Society, 2007, 154, B288.	1.3	34
220	Synthesis of nanorods and nanowires using biomolecules under conventional- and microwave-hydrothermal conditions. Journal of Materials Science, 2008, 43, 2377-2386.	1.7	34
221	CdS Nanorod-Based Structures: From Two- and Three-Dimensional Leaves to Flowers. Journal of Physical Chemistry C, 2008, 112, 13359-13365.	1.5	34
222	MXene/WS ₂ hybrids for visible-light-activated NO ₂ sensing at room temperature. Chemical Communications, 2021, 57, 9136-9139.	2.2	34
223	Detection of Nonequivalent Si Sites in Sepiolite and Palygorskite by Solid-state 29Si Magic Angle Spinning-Nuclear Magnetic Resonance. Clays and Clay Minerals, 1986, 34, 99-102.	0.6	34
224	Phillipsite in Cs Decontamination and Immobilization. Clays and Clay Minerals, 1985, 33, 145-151.	0.6	33
225	Porous silicon oxycarbide glasses from organically modified silica gels of high surface area. Journal of Sol-Gel Science and Technology, 1994, 1, 141-151.	1.1	33
226	Hydrothermal and microwave-hydrothermal preparation of silica gels. Materials Letters, 1996, 27, 313-315.	1.3	33
227	Novel honeycomb structure: a microporous ZSM-5 and macroporous mullite composite. Journal of Materials Chemistry, 1998, 8, 2327-2329.	6.7	33
228	Processing of Pb(Zr0.52Ti0.48)O3 (PZT) ceramics from microwave and conventional hydrothermal powders. Materials Research Bulletin, 1999, 34, 1411-1419.	2.7	33
229	Anionic Clays as Potential Slow-Release Fertilizers: Nitrate Ion Exchange. Journal of Porous Materials, 2003, 10, 243-248.	1.3	33
230	Magnetite syntheses from room temperature to 150°C with and without microwaves. Ceramics International, 2012, 38, 2563-2568.	2.3	33
231	Phenol and/or Zn2+ adsorption by single- or dual-cation organomontmorillonites. Applied Clay Science, 2017, 140, 1-9.	2.6	33
232	Flexible room-temperature formaldehyde sensors based on rGO film and rGo/MoS ₂ hybrid film. Nanotechnology, 2017, 28, 325501.	1.3	33
233	Spinel-type cobalt-manganese oxide catalyst for degradation of Orange II using a novel heterogeneous photo-chemical catalysis system. Ceramics International, 2018, 44, 19474-19480.	2.3	33
234	TiO2@g-C3N4 core/shell spheres with uniform mesoporous structures for high performance visible-light photocatalytic application. Ceramics International, 2019, 45, 18844-18851.	2.3	33

#	Article	IF	CITATIONS
235	Anode electrodeposition of 3D mesoporous Fe2O3 nanosheets on carbon fabric for flexible solid-state asymmetric supercapacitor. Ceramics International, 2019, 45, 10420-10428.	2.3	33
236	Grain orientation in sol-gel derived Ln2Ti2O7 ceramics (Ln = La, Nd). Materials Letters, 1991, 12, 306-310.	1.3	32
237	Occlusion of KNO3 and NH4NO3 in natural zeolites. Zeolites, 1997, 18, 171-175.	0.9	32
238	Crystallization of ThSiO ₄ from structurally and/or compositionally diphasic gels. Journal of Materials Research, 1987, 2, 489-493.	1.2	31
239	Kinetics, equilibria and thermodynamics of ion exchange in substituted tobermorites. Materials Research Bulletin, 1989, 24, 311-320.	2.7	31
240	Microwave-hydrothermal synthesis of barium titanate under stirring condition. Ceramics International, 2010, 36, 1165-1169.	2.3	31
241	Anomalous but massive removal of two organic dye pollutants simultaneously. Journal of Hazardous Materials, 2016, 318, 54-60.	6.5	31
242	Liquid–Liquid Microextraction of Cu ²⁺ from Water Using a New Circle Microchannel Device. Industrial & Engineering Chemistry Research, 2017, 56, 12717-12725.	1.8	31
243	Bisulfite assisted photocatalytic degradation of methylene blue by Ni-Fe-Mn oxide from MnO4 intercalated LDH. Applied Clay Science, 2018, 161, 235-241.	2.6	31
244	Mechanical activation of zero-valent iron (ZVI) in the presence of CaCO3: Improved reactivity of ZVI for enhancing As(III) removal from water. Journal of Cleaner Production, 2021, 286, 124926.	4.6	31
245	Strategies to Develop Earthâ€Abundant Heterogeneous Oxygen Evolution Reaction Catalysts for pHâ€Neutral or pHâ€Nearâ€Neutral Electrolytes. Small Methods, 2021, 5, e2000719.	4.6	31
246	Significantly improved conductivity of spinel Co ₃ O ₄ porous nanowires partially substituted by Sn in tetrahedral sites for high-performance quasi-solid-state supercapacitors. Journal of Materials Chemistry A, 2021, 9, 7005-7017.	5.2	31
247	Preparation of a diphasic photosensitive xerogel. Journal of Materials Science Letters, 1984, 3, 439-442.	0.5	30
248	Controlled crystallization of vaterite from viscous solutions of organic colloids. Journal of Materials Research, 1990, 5, 2928-2932.	1.2	30
249	Sol-gel processing of oriented PbTiO3 thin films with lead acetylacetonate as the lead precursor. Materials Letters, 1994, 20, 71-74.	1.3	30
250	Ammonium Nitrate Occlusion vs. Nitrate Ion Exchange in Natural Zeolites. Soil Science Society of America Journal, 1998, 62, 1455-1459.	1.2	30
251	Na-4-mica: simplified synthesis from kaolinite, characterization and Zn, Cd, Pb, Cu and Ba uptake kinetics. Journal of Materials Chemistry, 2000, 10, 1649-1653.	6.7	30
252	Selenium oxyanions: Highly selective uptake by a novel anion exchanger. Journal of Materials Research, 2002, 17, 2993-2996.	1.2	30

#	Article	IF	CITATIONS
253	On-chip grown ZnO nanosheet-array with interconnected nanojunction interfaces for enhanced optoelectronic NO2 gas sensing at room temperature. Journal of Colloid and Interface Science, 2019, 554, 19-28.	5.0	30
254	Degradation of dye in wastewater by Homogeneous Fe(VI)/NaHSO3 system. Chemosphere, 2019, 228, 595-601.	4.2	30
255	Role of Montmorillonite, Kaolinite, or Illite in Pyrite Flotation: Differences in Clay Behavior Based on Their Structures. Langmuir, 2020, 36, 10860-10867.	1.6	30
256	Catalytic degradation of methylene blue through activation of bisulfite with CoO nanoparticles. Separation and Purification Technology, 2020, 239, 116561.	3.9	30
257	Structural Differences in Mullite Xerogels from Different Precursors Characterized by 27Al and 29Si MASNMR. Journal of Solid State Chemistry, 1993, 106, 73-82.	1.4	29
258	High surface area SiC/silicon oxycarbide glasses prepared from phenyltrimethoxysilane-tetramethoxysilane gels. Journal of Porous Materials, 1996, 2, 245-252.	1.3	29
259	Formation of Novel ZSMâ€5/Porous Mullite Composite from Sintered Kaolin Honeycomb by Hydrothermal Reaction. Journal of the American Ceramic Society, 2000, 83, 1093-1097.	1.9	29
260	Highly efficient visible light degradation of Rhodamine B by nanophasic Ag3PO4 dispersed on SBA-15. Microporous and Mesoporous Materials, 2014, 193, 154-159.	2.2	29
261	Heterogeneous activation of persulfate by Mg doped Ni(OH)2 for efficient degradation of phenol. Chemosphere, 2022, 286, 131647.	4.2	29
262	UV-activated WS2/SnO2 2D/0D heterostructures for fast and reversible NO2 gas sensing at room temperature. Sensors and Actuators B: Chemical, 2022, 364, 131903.	4.0	29
263	Hydrothermal Reaction and Dissolution Studies of CsAlSi5Or12 in Water and Brines. Journal of the American Ceramic Society, 1983, 66, 471-474.	1.9	28
264	Anomalous microwave melting of zeolites. Materials Letters, 1986, 4, 107-110.	1.3	28
265	Gelling properties of sepiolite versus montmorillonite. Applied Clay Science, 1988, 3, 165-176.	2.6	28
266	Germanium accumulation and toxicity in barley. Journal of Plant Nutrition, 1995, 18, 1417-1426.	0.9	28
267	Microwave–hydrothermal decomposition of chlorinated organic compounds. Materials Letters, 2000, 43, 259-263.	1.3	28
268	Microwave-hydrothermal synthesis of Al-substituted tobermorite from zeolites. Materials Research Bulletin, 2002, 37, 1025-1032.	2.7	28
269	Highly Charged Swelling Mica Reduces Free and Extractable Cu Levels in Cu-Contaminated Soils. Environmental Science & Technology, 2008, 42, 9197-9202.	4.6	28
270	Titanosilicates: Giant exchange capacity and selectivity for Sr and Ba. Separation and Purification Technology, 2012, 95, 222-226.	3.9	28

#	Article	IF	CITATIONS
271	Synthesis of p-n heterojunction Ag3PO4/NaTaO3 composite photocatalyst for enhanced visible-light-driven photocatalytic performance. Materials Letters, 2019, 251, 192-195.	1.3	28
272	Antimicrobial activity of X zeolite exchanged with Cu2+ and Zn2+ on Escherichia coli and Staphylococcus aureus. Environmental Science and Pollution Research, 2019, 26, 2782-2793.	2.7	28
273	Hydrothermal Reactions of Clay Minerals and Shales with Cesium Phases from Spent Fuel Elements. Clays and Clay Minerals, 1981, 29, 299-308.	0.6	27
274	Epitaxial Crystallization of Seeded Albite Glass. Journal of the American Ceramic Society, 1991, 74, 1378-1381.	1.9	27
275	Alkali metal and alkaline earth metal ion exchange with Naâ€4â€mica prepared by a new synthetic route from kaolinite. Journal of Materials Chemistry, 1999, 9, 2475-2479.	6.7	27
276	Hydrothermal Synthesis OF Zn-smectites. Clays and Clay Minerals, 2002, 50, 299-305.	0.6	27
277	Synthesis and characterization of PSU-1, a novel cage-like mesoporous silicaElectronic supplementary information (ESI) available: X-ray diffraction patterns for uncalcined (Fig. 1s), calcined (Fig. 2s) and hydrothermally treated (Fig. 3s) samples of PSU-1. See http://www.rsc.org/suppdata/jm/b3/b303406b/. Journal of Materials Chemistry, 2003, 13, 1710.	6.7	27
278	Rapid Synthesis of Monodispersed .ALPHAFe2O3 Nanoparticles from Fe(NO3)3 Solution by Microwave Irradiation. Journal of the Ceramic Society of Japan, 2004, 112, 384-387.	1.3	27
279	Multi-level assemblies of lead sulphide nanorods. Nanotechnology, 2006, 17, 2574-2580.	1.3	27
280	Solvothermal/ Hydrothermal Synthesis of Metal Oxides and Metal Powders with and without Microwaves. Zeitschrift Fur Naturforschung - Section B Journal of Chemical Sciences, 2010, 65, 1033-1037.	0.3	27
281	Micro-nanostructured δ-Bi2O3 with surface oxygen vacancies as superior adsorbents for SeOx2â^' ions. Journal of Hazardous Materials, 2018, 360, 279-287.	6.5	27
282	Crystallization of Anorthite-Seeded Albite Glass by Solid-State Epitaxy. Journal of the American Ceramic Society, 1992, 75, 2665-2670.	1.9	26
283	Sol-gel processing of oriented SrTiO3 thin films. Materials Letters, 1995, 23, 123-127.	1.3	26
284	Infrared Emission Spectroscopic Study of the Dehydroxylation via Surface Silanol Groups of Synthetic and Natural Beidellite. Journal of Colloid and Interface Science, 1999, 212, 562-569.	5.0	26
285	Microwave-assisted polyol synthesis of Ag powders. Journal of Materials Research, 2003, 18, 747-750.	1.2	26
286	Alkaline earth cation exchange with novel Na-3-mica: kinetics and thermodynamic selectivities. Journal of Materials Chemistry, 2004, 14, 1031.	6.7	26
287	Conventional- and microwave-hydrothermal synthesis of LiMn2O4: Effect of synthesis on electrochemical energy storage performances. Ceramics International, 2014, 40, 3155-3163.	2.3	26
288	Capture of radioactive cations from water using niobate nanomaterials with layered and tunnel structures. RSC Advances, 2015, 5, 75354-75359.	1.7	26

#	Article	IF	CITATIONS
289	High-yield production of mesoporous nanoscrolls from kaolinite by ultrasonic assisted exfoliation. Microporous and Mesoporous Materials, 2017, 241, 66-71.	2.2	26
290	In situ hydrothermal preparation of mesoporous Fe 3 O 4 film for high-performance negative electrodes of supercapacitors. Microporous and Mesoporous Materials, 2018, 265, 189-194.	2.2	26
291	Enhancement of photo-fenton-like degradation of orange II by MnO2/NiO nanocomposite with the synergistic effect from bisulfite. Journal of Alloys and Compounds, 2019, 785, 343-349.	2.8	26
292	Emulsions stabilized by highly hydrophilic TiO2 nanoparticles via van der Waals attraction. Journal of Colloid and Interface Science, 2021, 589, 378-387.	5.0	26
293	Hydrothermal Effects on Cesium Sorption and Fixation by Clay Minerals and Shales. Clays and Clay Minerals, 1980, 28, 142-148.	0.6	25
294	Hydrothermal preparation of the low-expansion NZP family of materials. International Journal of High Technology Ceramics, 1988, 4, 31-39.	0.2	25
295	Synthetic Clay Excels in 90Sr Removal. Journal of Materials Research, 2000, 15, 1254-1256.	1.2	25
296	Microwave-hydrothermal synthesis and characterization of microporous–mesoporous disordered silica using mixed-micellar-templating approach. Microporous and Mesoporous Materials, 2004, 73, 161-170.	2.2	25
297	Influence of mesoporosity on the sorption of 2,4-dichlorophenoxyacetic acid onto alumina and silica. Journal of Colloid and Interface Science, 2004, 272, 10-20.	5.0	25
298	Rapid Microwave-Hydrothermal Synthesis of Anatase Form of Titanium Dioxide. Journal of the American Ceramic Society, 2005, 88, 3238-3240.	1.9	25
299	In situ growth of silicon carbide nanowires from anthracite surfaces. Ceramics International, 2011, 37, 1063-1072.	2.3	25
300	Hierarchical SAPO-11 preparation in the presence of glucose. Materials Letters, 2015, 154, 116-119.	1.3	25
301	Nanoseed-assisted rapid formation of ultrathin ZnO nanorods for efficient room temperature NO2 detection. Ceramics International, 2016, 42, 15876-15880.	2.3	25
302	Charging mechanism analysis of macerals during triboelectrostatic enrichment process: Insights from relative dielectric constant, specific resistivity and X-ray diffraction. Fuel, 2018, 225, 533-541.	3.4	25
303	Highly sensitive, fast and reversible NO2 sensors at room-temperature utilizing nonplasmonic electrons of ZnO/Pd hybrids. Ceramics International, 2020, 46, 8462-8468.	2.3	25
304	Degradation of orange II by Fe@Fe2O3 core shell nanomaterials assisted by NaHSO3. Chemosphere, 2020, 244, 125588.	4.2	25
305	Cesium Sorption and Desorption Behavior of Kaolinites. Soil Science Society of America Journal, 1978, 42, 531-532.	1.2	25
306	Single-phase and diphasic aerogels and xerogels of mullite: Preparation and characterization. Journal of the European Ceramic Society, 1996, 16, 143-147.	2.8	24

#	Article	IF	CITATIONS
307	Selective Cu2+and Pb2+Exchange with Highly Charged Cation Exchanger of Na-4-Mica. Separation Science and Technology, 1999, 34, 2275-2292.	1.3	24
308	In situ transformation of geopolymer gels to self-supporting NaX zeolite monoliths with excellent compressive strength. Microporous and Mesoporous Materials, 2018, 261, 164-169.	2.2	24
309	Persulfate activation by MnCuS nanocomposites for degradation of organic pollutants. Separation and Purification Technology, 2021, 261, 118290.	3.9	24
310	Sol-gel thin films of SrTiO3 from chemically modified alkoxide precursors. Materials Letters, 1991, 12, 311-315.	1.3	23
311	Porous mullite honeycomb by hydrothermal treatment of fired kaolin bodies in NaOH. Journal of Porous Materials, 1996, 2, 299-305.	1.3	23
312	A Synthetic Na-Rich Mica: Synthesis and Characterization by 27Al and 29Si Magic Angle Spinning Nuclear Magnetic Resonance Spectroscopy. Clays and Clay Minerals, 1999, 47, 410-416.	0.6	23
313	pH dependent coprecipitated oxalate precursors – a thermal study of barium titanate. Materials Letters, 1999, 39, 359-363.	1.3	23
314	Swelling mica-type clays: synthesis by NaCl melt method, NMR characterization and cation exchange selectivity. Journal of Materials Chemistry, 2005, 15, 4241.	6.7	23
315	Microwave-hydrothermal synthesis of Fe-based materials for lithium-ion batteries and supercapacitors. Ceramics International, 2014, 40, 2877-2884.	2.3	23
316	Facile synthesis of nanorods of tetragonal barium titanate using ethylene glycol. Ceramics International, 2015, 41, 5581-5587.	2.3	23
317	Ligand-directed rapid formation of ultralong ZnO nanowires by oriented attachment for UV photodetectors. Journal of Materials Chemistry C, 2016, 4, 5755-5765.	2.7	23
318	An efficient SO2-adsorbent from calcination of natural magnesite. Ceramics International, 2017, 43, 12557-12562.	2.3	23
319	A comparative study of synthetic tubular kaolinite nanoscrolls and natural halloysite nanotubes. Applied Clay Science, 2019, 168, 421-427.	2.6	23
320	Bi2MoO6 microspheres for the degradation of orange II by heterogeneous activation of persulfate under visible light. Materials Letters, 2020, 261, 127099.	1.3	23
321	Three-dimensional stretchable fabric-based electrode for supercapacitors prepared by electrostatic flocking. Chemical Engineering Journal, 2020, 390, 124442.	6.6	23
322	Metallic nickel–cobalt phosphide/multilayer graphene composite for high-performance supercapacitors. New Journal of Chemistry, 2020, 44, 8796-8804.	1.4	23
323	Powder x-ray diffraction study of a cryptomelane-type manganic acid and its alkali cation exchanged forms. Journal of Materials Research, 1993, 8, 3145-3150.	1.2	22
324	Seeding Effects on Crystallization of KAlSi3O8, RbAlSi3O8, and CsAlSi3O8 Gels and Classes. Journal of the American Ceramic Society, 1994, 77, 3105-3112.	1.9	22

#	Article	IF	CITATIONS
325	Sequestration of Cesium and Strontium by Tobermorite Synthesized from Fly Ashes. Journal of the American Ceramic Society, 1996, 79, 1707-1710.	1.9	22
326	Mn-smectites: Hydrothermal synthesis and characterization. Applied Clay Science, 2007, 38, 104-112.	2.6	22
327	Evaluation of Volatile Hydrocarbon Emission Characteristics of Carbonaceous Additives in Green Sand Foundries. Environmental Science & Technology, 2007, 41, 2957-2963.	4.6	22
328	As-synthesized MCM-41 silica: new adsorbent for perchlorate. Journal of Porous Materials, 2010, 17, 651-656.	1.3	22
329	Synthesis of Fe2O3–NiO–Cr2O3 composites from NiFe-layered double hydroxide for degrading methylene blue under visible light. Applied Clay Science, 2015, 107, 85-89.	2.6	22
330	Experimental and Theoretical Studies of Methyl Orange Uptake by Mn–Rich Synthetic Mica: Insights into Manganese Role in Adsorption and Selectivity. Nanomaterials, 2020, 10, 1464.	1.9	22
331	Cesium sorption by clay minerals and shales at elevated temperatures. Journal of Inorganic and Nuclear Chemistry, 1979, 41, 397-400.	0.5	21
332	Al-substituted tobermorite—The coordination of aluminum as revealed by solid-state 27Al magic angle spinning (MAS) NMR. Cement and Concrete Research, 1985, 15, 723-728.	4.6	21
333	Microstructure and mechanical properties of synthetic opal: A chemically bonded ceramic. Journal of Materials Research, 1986, 1, 667-674.	1.2	21
334	Mechanisms of Palygorskite and Sepiolite Alteration as Deduced from Solid-State 27Al and 29Si Nuclear Magnetic Resonance Spectroscopy. Clays and Clay Minerals, 1989, 37, 469-473.	0.6	21
335	Mercury(II) Exchange by Highly Charged Swelling Micas, Sodium Engelhard Titanosilicate-4, and Sodium Titanosilicate. Environmental Science & Technology, 2011, 45, 6954-6960.	4.6	21
336	Clover leaf-shaped Al2O3 extrudate as a support for high-capacity and cost-effective CO2 sorbent. Journal of Hazardous Materials, 2011, 192, 1505-1508.	6.5	21
337	Tribocharging of macerals with various materials: Role of surface oxygen-containing groups and potential difference of macerals. Fuel, 2018, 233, 759-768.	3.4	21
338	Reduction of copper acetate hydroxide hydrate interlayers in montmorillonite by a polyol process. A new approach in the preparation of metal-supported catalysts. Journal of Materials Chemistry, 1992, 2, 559.	6.7	20
339	Some significant advances in sol-gel processing of dense structural ceramics. Journal of Sol-Gel Science and Technology, 1996, 6, 127-138.	1.1	20
340	Removal of Lead lons Using Porous Hydroxyapatite Monoliths Synthesized from Gypsum Waste Journal of the Ceramic Society of Japan, 2000, 108, 315-317.	1.3	20
341	NMR Study of Strontium Binding by a Micaceous Mineral. Journal of Physical Chemistry B, 2006, 110, 7159-7164.	1.2	20
342	Organosilicas and organo-clay minerals as sorbents for toluene. Applied Clay Science, 2011, 52, 184-189.	2.6	20

#	Article	IF	CITATIONS
343	Facile synthesis of highly branched poly(acrylonitrile-co-vinyl acetate)s with low viscosity and high thermal stability via radical aqueous solution polymerization. Polymer Chemistry, 2014, 5, 3326-3334.	1.9	20
344	Surfactant-assisted synthesis of ZIF-8 nanocrystals for phthalic acid adsorption. Journal of Sol-Gel Science and Technology, 2016, 80, 523-530.	1.1	20
345	Ni and Co doped yolk-shell type Fe 2 O 3 hollow microspheres as anode materials for lithium-ion batteries. Materials Chemistry and Physics, 2018, 211, 452-461.	2.0	20
346	Synergic enhancement of the anticorrosion properties of an epoxy coating by compositing with both graphene and halloysite nanotubes. Journal of Applied Polymer Science, 2019, 136, 47562.	1.3	20
347	Shale as a radioactive waste repository: the importance of vermiculite. Journal of Inorganic and Nuclear Chemistry, 1979, 41, 1793-1796.	0.5	19
348	Characterization of Synthetic and Naturally Occurring Clays by 27Al and 29Si Magic-Angle Spinning NMR Spectroscopy. Journal of the American Ceramic Society, 1986, 69, C-45-C-47.	1.9	19
349	An Extended Method for Analytical Evaluation of Distribution Coefficients on Selective Inorganic Ion Exchangers. Separation Science and Technology, 1992, 27, 813-821.	1.3	19
350	ION-EXCHANGE SELECTIVITY FOR ALKALI METAL IONS ON A CRYPTOMELANE-TYPE HYDROUS MANGANESE DIOXIDE. Solvent Extraction and Ion Exchange, 1993, 11, 143-158.	0.8	19
351	Nanophase ferrites for CO2 greenhouse gas decomposition. Journal of Materials Chemistry, 1997, 7, 2339-2340.	6.7	19
352	Crystal-size control and characterization of Na-4-mica prepared from kaolinite. Journal of Materials Chemistry, 2001, 11, 1222-1227.	6.7	19
353	Ultrafine Na-4-mica:Â Uptake of Alkali and Alkaline Earth Metal Cations by Ion Exchange. Langmuir, 2004, 20, 4920-4925.	1.6	19
354	Highly Charged Swelling Mica-Type Clays for Selective Cu Exchange. Environmental Science & Technology, 2008, 42, 113-118.	4.6	19
355	Co3O4/CoO ceramic catalyst: Bisulfite assisted catalytic degradation of methylene blue. Ceramics International, 2021, 47, 27617-27623.	2.3	19
356	Efficient degradation of orange II by core shell CoFe2O4–CeO2 nanocomposite with the synergistic effect from sodium persulfate. Chemosphere, 2022, 291, 132765.	4.2	19
357	Degradation of tetracycline by activating persulfate using biochar-based CuFe2O4 composite. Environmental Science and Pollution Research, 2022, 29, 67003-67013.	2.7	19
358	Efficient activation of persulfate by C@Fe3O4 in visible-light for tetracycline degradation. Chemosphere, 2022, 306, 135635.	4.2	19
359	Microwave-hydrothermal/solvothermal synthesis of kesterite, an emerging photovoltaic material. Ceramics International, 2014, 40, 1985-1992.	2.3	18
360	Highly mesoporous LaNiO 3 /NiO composite with high specific surface area as a battery-type electrode. Ceramics International, 2017, 43, 5687-5692.	2.3	18

#	Article	IF	CITATIONS
361	Selective removal of methyl orange and Cr anionic contaminants from mixed wastewater by in-situ formation of Zn-Al layered double hydroxides. Applied Clay Science, 2018, 161, 1-5.	2.6	18
362	Ultrafast microwave-hydrothermal synthesis of hexagonal plates of hematite. Materials Chemistry and Physics, 2018, 205, 210-216.	2.0	18
363	Hydrothermal synthesis of nano-kaolinite from K-feldspar. Ceramics International, 2018, 44, 15611-15617.	2.3	18
364	Fabrication and characterization of TiO2/Sepiolite nanocomposites doped with rare earth ions. Materials Letters, 2018, 228, 100-103.	1.3	18
365	Electrochemical behavior of representative electrode materials in artificial seawater for fabricating supercapacitors. Electrochimica Acta, 2019, 318, 211-219.	2.6	18
366	Hydrothermal interactions of basalts with Cs and Sr of spent fuel elements. Journal of Inorganic and Nuclear Chemistry, 1981, 43, 1967-1975.	0.5	17
367	Synthesis of LiAl2(OH)6+ intercalated montmorillonite by a hydrothermal soft chemical reaction. Journal of Materials Chemistry, 2000, 10, 483-488.	6.7	17
368	Role of framework on NH4NO3 occlusion in zeolite pores. Microporous and Mesoporous Materials, 2001, 50, 91-99.	2.2	17
369	Modification of Porous Silica with Activated Carbon and its Application for Fixation of Yeasts. Journal of Porous Materials, 2001, 8, 43-48.	1.3	17
370	Characteristics of nitrogen release from synthetic zeolite Na-P1 occluding NH4NO3. Journal of Controlled Release, 2005, 106, 44-50.	4.8	17
371	Synthesis of Pt Nanoparticles and Nanorods by Microwave-assisted Solvothermal Technique. Zeitschrift Fur Naturforschung - Section B Journal of Chemical Sciences, 2006, 61, 1566-1572.	0.3	17
372	Thermal decomposition behavior and de-intercalation mechanism of acetamide intercalated into kaolinite by thermoanalytical techniques. Applied Clay Science, 2015, 114, 309-314.	2.6	17
373	Role of Hydrothermal parameters on phase purity of orthorhombic LiMnO2 for use as cathode in Li ion battery. Ceramics International, 2015, 41, 6729-6733.	2.3	17
374	Flexible and internal series-connected supercapacitors with high working voltage using ultralight porous carbon nanofilms. Journal of Power Sources, 2017, 342, 762-771.	4.0	17
375	CO2 Adsorption by Several Types of Pillared Montmorillonite Clays. Applied Petrochemical Research, 2018, 8, 173-177.	1.3	17
376	Decolorization of methyl orange by MnO2/organic acid system: The role of Mn(III). Materials Research Bulletin, 2020, 122, 110670.	2.7	17
377	Sustainable electrochemical dyeing of indigo with Fe(â…¡)-based complexes. Journal of Cleaner Production, 2020, 276, 123251.	4.6	17
378	Activation of K2S2O8 by Ni–Ce composite oxides for the degradation of orange II with visible light assistance. Materials Chemistry and Physics, 2021, 270, 124784.	2.0	17

#	Article	IF	CITATIONS
379	Effect of layer charge and heat treatment on Cs fixation by layer silicate minerals. Journal of Inorganic and Nuclear Chemistry, 1978, 40, 893-896.	0.5	16
380	Hydrothermal Transformations in Candidate Overpack Materials and their Effects on Cesium and Strontium Sorption. Nuclear Technology, 1981, 54, 118-122.	0.7	16
381	Alteration of Clay Minerals and Zeolites in Hydrothermal Brines. Clays and Clay Minerals, 1983, 31, 383-390.	0.6	16
382	Composites of MCM-41 silica with rice husk: hydrothermal synthesis, characterisation and application for perchlorate separation. Materials Research Innovations, 2010, 14, 351-354.	1.0	16
383	The effect of Si/Al ratio and moisture on an organic/inorganic hybrid material: Thioindigo/montmorillonite. Applied Clay Science, 2011, 51, 61-67.	2.6	16
384	Organoclays of high-charge synthetic clays and alumina pillared natural clays: Perchlorate uptake. Applied Clay Science, 2013, 80-81, 340-345.	2.6	16
385	Simultaneous removal of Zn2+ and p-nitrophenol from wastewater using nanocomposites of montmorillonite with alkyl-ammonium and complexant. Environmental Research, 2021, 201, 111496.	3.7	16
386	Porous N-doped carbon nanospheres with encapsulated cobalt nanocrystals for persulfate activation to degrade tetracycline. Ceramics International, 2022, 48, 27622-27630.	2.3	16
387	Synthesis and characterization of a 12. 6Ã calcium silicate hydrate. Cement and Concrete Research, 1986, 16, 580-586.	4.6	15
388	Uptake of cadmium, copper, and lead by microporous synthetic Na-birnessite. Journal of Porous Materials, 2011, 18, 125-131.	1.3	15
389	Microwave-hydrothermal synthesis of extremely high specific surface area anatase for decomposing NOx. Ceramics International, 2012, 38, 6099-6105.	2.3	15
390	High Surface Area Activated Carbon Synthesized from Bio-Based Material for Supercapacitor Application. Nanoscience and Nanotechnology Letters, 2014, 6, 997-1000.	0.4	15
391	Detailed investigation of N-doped microporous carbons derived from urea furfural resin for CO2 capture. Journal of Porous Materials, 2015, 22, 1663-1672.	1.3	15
392	Synthesis and photocatalytic properties of new ternary Ni–Fe–Cr hydrotalcite-like compounds. Ceramics International, 2016, 42, 15981-15988.	2.3	15
393	Synthesis of mesoporous carbons with narrow pore size distribution from metal-organic framework MIL-100(Fe). Microporous and Mesoporous Materials, 2016, 234, 162-165.	2.2	15
394	Porous Ag-doped MnO2 thin films for supercapacitor electrodes. Journal of Porous Materials, 2017, 24, 1717-1723.	1.3	15
395	Fe–Co-SBA assisted by visible light can effectively activate NaHSO3 or H2O2 for enhanced degradation of Orange â…;: Activation of NaHSO3 versus H2O2. Microporous and Mesoporous Materials, 2021, 315, 110902.	2.2	15
396	Recent advances in Co-based co-catalysts for efficient photocatalytic hydrogen generation. Journal of Colloid and Interface Science, 2022, 608, 1553-1575.	5.0	15

#	Article	IF	CITATIONS
397	Persulfate activation of CuS@Ti3C2-based MXene with Bi-active centers toward Orange II removal under visible light. Colloids and Surfaces A: Physicochemical and Engineering Aspects, 2022, 648, 129315.	2.3	15
398	Mechanisms of Advanced Oxidation Processing on Bentonite Consumption Reduction in Foundry. Environmental Science & Technology, 2005, 39, 7712-7718.	4.6	14
399	Gluconate controls one-dimensional growth of tellurium nanostructures. Journal of Materials Research, 2006, 21, 343-348.	1.2	14
400	Binding Waste Anthracite Fines with Si-Containing Materials as an Alternative Fuel for Foundry Cupola Furnaces. Environmental Science & Technology, 2011, 45, 3062-3068.	4.6	14
401	Suppression of NH3 and N2O emissions by massive urea intercalation in montmorillonite. Journal of Soils and Sediments, 2011, 11, 416-422.	1.5	14
402	Synthesis of PZT fine particles using Ti3+ precursor at a low hydrothermal temperature of 110°C. Ceramics International, 2011, 37, 1101-1107.	2.3	14
403	Nanolayered tin phosphate: a remarkably selective Cs ion sieve for acidic waste solutions. Chemical Communications, 2015, 51, 15661-15664.	2.2	14
404	Kinetics and thermodynamic analysis of the adsorption of hydroxy-Al cations by montmorillonite. Applied Clay Science, 2016, 129, 79-87.	2.6	14
405	Polymer-coal composite as a novel plastic material. Materials Letters, 2017, 197, 31-34.	1.3	14
406	Green synthesis of nano-muscovite and niter from feldspar through accelerated geomimicking process. Applied Clay Science, 2018, 165, 71-76.	2.6	14
407	Sol-Gel Synthesis of Strontium Pyroniobate and Calcium Pyroniobate. Journal of the American Ceramic Society, 1992, 75, 2697-2701.	1.9	13
408	Simplified Synthesis of Na-4-Mica from Kaolinite and Its Cation-Exchange Properties. Separation Science and Technology, 2000, 35, 1133-1152.	1.3	13
409	Uptake of cadmium by synthetic mica and apatite: Observation by micro-PIXE. Nuclear Instruments & Methods in Physics Research B, 2003, 210, 513-518.	0.6	13
410	Nanoparticles of Pd: Synthesis by Microwave-Solvothermal Method and Optical Properties. Journal of Nanoscience and Nanotechnology, 2008, 8, 3930-3935.	0.9	13
411	Effect of particle size on cesium exchange kinetics by K-depleted phlogopite. Applied Clay Science, 2009, 43, 401-407.	2.6	13
412	Hydronium-Promoted Equilibrium Mechanism for the Alkali Metal Cation Exchange Reaction in Na-4-Mica. Journal of Physical Chemistry C, 2012, 116, 18678-18683.	1.5	13
413	Nanocomposite synthesis and characterization of Kesterite, Cu2ZnSnS4 (CZTS) for photovoltaic applications. Ceramics International, 2013, 39, 7935-7941.	2.3	13
414	Producing petrochemicals from catalytic fast pyrolysis of corn fermentation residual by-products generated from citric acid production. Renewable Energy, 2016, 89, 331-338.	4.3	13

#	Article	IF	CITATIONS
415	Facile fabrication of freestanding three-dimensional composites for supercapacitors. Chemical Communications, 2016, 52, 2691-2694.	2.2	13
416	Mineralogy controls on reactive transport of Marcellus Shale waters. Science of the Total Environment, 2018, 630, 1573-1582.	3.9	13
417	Highly efficient removal of antimonite (Sb (III)) from aqueous solutions by organoclay and organozeolite: Kinetics and Isotherms. Applied Clay Science, 2021, 203, 106004.	2.6	13
418	Mineral-Based Slow Release Fertilizers: A Review. Han'guk T'oyang Piryo Hakhoe Chi Han'guk T'oyang Piryo Hakhoe, 2015, 48, 1-7.	0.1	13
419	Alteration of CsAlSiO4 in hydrothermal fluids. Nuclear and Chemical Waste Management, 1982, 3, 169-172.	0.2	12
420	Hydrothermal Reactions of Strontium and Transuranic Simulator Elements with Clay Minerals, Zeolites, and Shales. Clays and Clay Minerals, 1983, 31, 113-121.	0.6	12
421	Intercalated metal-clay catalysts in direct liquefaction of bituminous coal. Energy & Fuels, 1993, 7, 430-431.	2.5	12
422	Cesium selectivity of (Al+Na)-substituted tobermorite. Cement and Concrete Research, 1994, 24, 573-579.	4.6	12
423	Sol-gel processing of piezoelectric thin films. Ferroelectrics, 1999, 232, 191-195.	0.3	12
424	Synthesis of Na-2-mica from talc and kaolinite: characterization and Sr2+ uptake. Journal of Materials Chemistry, 2003, 13, 377-381.	6.7	12
425	Composite Proton Conductive Membranes for Elevated Temperature and Reduced Relative Humidity PEMFC. ECS Transactions, 2009, 25, 1141-1150.	0.3	12
426	Mn-kaolinite synthesis under low-temperature hydrothermal conditions. Applied Clay Science, 2009, 44, 237-241.	2.6	12
427	Proton Conductive Inorganic Materials for Temperatures Up to 120°C and Relative Humidity Down to 5%. Journal of the Electrochemical Society, 2010, 157, B1634.	1.3	12
428	Composite Membranes with Sulfonic and Phosphonic Functionalized Inorganics for Reduced Relative Humidity PEM Fuel Cells. Journal of the Electrochemical Society, 2011, 158, B690-B697.	1.3	12
429	Massive Intercalation of Urea in Montmorillonite. Soil Science Society of America Journal, 2011, 75, 2361-2366.	1.2	12
430	Adsorbate-dependent uptake behavior of topographically bi-functionalized ordered mesoporous silica materials. Journal of Porous Materials, 2015, 22, 1297-1303.	1.3	12
431	Novel inorganic tin phosphate gel: multifunctional material. Chemical Communications, 2018, 54, 2682-2685.	2.2	12
432	Iron activated sodium bisulfite enhances generation of Mn (III) species through the MnO2/bisulfite catalytic process. Ceramics International, 2019, 45, 892-898.	2.3	12

#	Article	IF	CITATIONS
433	Comparison of Cation Exchange in Ganophyllite and [Na + Al]-Substituted Tobermorite: Crystal-Chemical Implications. Mineralogical Magazine, 1988, 52, 371-375.	0.6	12
434	Preliminary Characterization of Gel Precursors and Their High-Temperature Products by 27Al Magic-Angle Spinning NMR. Journal of the American Ceramic Society, 1985, 68, C-243-C-245.	1.9	11
435	The influence of water vapor on thermal transformation of boehmite. Journal of Materials Research, 1992, 7, 444-449.	1.2	11
436	Composite aerogels of silica and minerals of different morphologies. Materials Letters, 1994, 19, 221-224.	1.3	11
437	Carbon-silica xerogel and aerogel composites. Journal of Porous Materials, 1995, 1, 75-84.	1.3	11
438	Temperature-programmed desorption vs. N2 desorption in determining pore-size distribution of mesoporous silica molecular sieves. Journal of Porous Materials, 1996, 3, 115-119.	1.3	11
439	Conventional- versus microwave-hydrothermal leaching of glass from sintered kaolinite to make porous mullite. Journal of Porous Materials, 1996, 3, 127-131.	1.3	11
440	Synthesis and characterization of hexagonally packed mesoporous tantalum oxide thin film. Materials Letters, 2002, 57, 444-447.	1.3	11
441	Highly charged swelling micas of different charge densities: Synthesis, characterization, and selectivity for Sr and Ba. Separation and Purification Technology, 2013, 104, 238-245.	3.9	11
442	Simultaneous arsenate and alkali removal from alkaline wastewater by in-situ formation of Zn–Al layered double hydroxide. Microporous and Mesoporous Materials, 2016, 227, 137-143.	2.2	11
443	Enhanced Cycling Stability through Erbium Doping of LiMn2O4 Cathode Material Synthesized by Sol-Gel Technique. Materials, 2018, 11, 1558.	1.3	11
444	Efficient degradation of orange II by ZnMn2O4 in a novel photo-chemical catalysis system. Frontiers of Chemical Science and Engineering, 2020, 14, 956-966.	2.3	11
445	Degradation of organic pollutants by ZnMn2O4/organic acid system: Identification of active species. Materials Letters, 2021, 293, 129725.	1.3	11
446	Stabilization of heavy metals from lead-zinc ore tailings with sodium diethyl dithiocarbamate functionalized montmorillonite (DDTC-Mt): Leaching characteristics and remediating mechanism. Minerals Engineering, 2022, 183, 107608.	1.8	11
447	Sintering of diphasic mullite gel. Journal of the European Ceramic Society, 1996, 16, 561-566.	2.8	10
448	A Microwave-assisted Method for the Rapid Removal of K From Phlogopite. Clays and Clay Minerals, 2002, 50, 248-253.	0.6	10
449	Synthesis and characterization of nickel–copper hydroxide acetate, NiCu(OH)3.1(OCOCH3)0.9·0.9H2O. Microporous and Mesoporous Materials, 2006, 89, 123-131.	2.2	10
450	Synthesis of Kaolinite from Micas and K-depleted Micas. Clays and Clay Minerals, 2007, 55, 565-571.	0.6	10

#	Article	IF	CITATIONS
451	Hydrothermal synthesis of Mn-kaolinite using NaOH or KOH and characterization. Applied Clay Science, 2010, 49, 74-79.	2.6	10
452	Sorption characteristics of lead cations on microporous organo-birnessite. Applied Clay Science, 2013, 83-84, 263-269.	2.6	10
453	Controlled synthesis of hexagonal α-Fe2O3 crystals for ceramic colors by hydrothermal reaction of FeCl3 and NaOH solutions. Ceramics International, 2017, 43, 14050-14056.	2.3	10
454	Synthesis of pore-expanded mesoporous ZIF-8/silica composites in the presence of swelling agent. Journal of Sol-Gel Science and Technology, 2017, 81, 268-275.	1.1	10
455	Immobilization mechanism of As, Mn, Pb and Zn ions in sulfide tailings by the addition of triethylenetetramine-montmorillonite nanocomposite. Chemical Engineering Journal, 2022, 435, 134817.	6.6	10
456	Leaching characteristics and stabilization of heavy metals in tin-polymetallic tailings by sodium diethyl dithiocarbamate intercalated montmorillonite (DDTC-Mt). Journal of Cleaner Production, 2022, 344, 131041.	4.6	10
457	Sol-gel fabrication of nanocomposites: Alternate thin layers of PbTiO3 and PbZrO3. Materials Research Bulletin, 1997, 32, 1091-1097.	2.7	9
458	Crystallization of Electrostatically Seeded Lanthanum Hexaluminate Films on Polycrystalline Oxide Fibers. Journal of the American Ceramic Society, 2000, 83, 3172-3178.	1.9	9
459	Microporous Semicrystalline Silica Materials. Journal of Materials Research, 2000, 15, 1437-1440.	1.2	9
460	Novel clays: Solid-state synthesis, characterization and cation exchange selectivity. Current Applied Physics, 2008, 8, 104-106.	1.1	9
461	ZSM-5 and ferrierite single crystals with lower Si/Al ratios: Synthesis and single-crystal synchrotron X-ray diffraction studies. Microporous and Mesoporous Materials, 2011, 143, 243-248.	2.2	9
462	Semi-continuous and fast synthesis of nanophase cubic BaTiO3 using a single-mode home-built microwave reactor. Materials Letters, 2012, 83, 8-10.	1.3	9
463	Microwave- or conventional–hydrothermal synthesis of Co-based materials for electrochemical energy storage. Ceramics International, 2014, 40, 8183-8188.	2.3	9
464	Light and Temperature as Dual Stimuli Lead to Self-Assembly of Hyperbranched Azobenzene-Terminated Poly(N-isopropylacrylamide). Polymers, 2016, 8, 183.	2.0	9
465	Selective sorption of strontium using two different types of nanostructured manganese oxides. Journal of Porous Materials, 2018, 25, 321-328.	1.3	9
466	Removal of Cu ²⁺ from Water Using Liquid‣iquid Microchannel Extraction. Chemical Engineering and Technology, 2020, 43, 974-982.	0.9	9
467	Heterogeneous activation of persulfate by Bi2MoO6–CuS composite for efficient degradation of orange II under visible light. Chemosphere, 2022, 293, 133558.	4.2	9
468	Efficient activation of K2S2O8 by MoS2-ZnFe2O4 composite for the rapid degradation of tetracycline. Materials Letters, 2022, 318, 132204.	1.3	9

#	Article	IF	CITATIONS
469	CDs@Cr2O3 catalytic degradation of Orange II based on non-radical pathway. Materials Chemistry and Physics, 2022, 287, 126257.	2.0	9
470	Molecular Engineering of Injectable, Fast Self-Repairing Hydrogels with Tunable Gelation Time: Characterization by Diffusing Wave Spectroscopy. Macromolecules, 2022, 55, 6474-6486.	2.2	9
471	Hydrothermal stability of β-Cs2U2O7 and SrZrO3 in fluids. Journal of Inorganic and Nuclear Chemistry, 1981, 43, 2833-2837.	0.5	8
472	Oxygen Isotope Changes during Mica Alteration. Clays and Clay Minerals, 1985, 33, 214-218.	0.6	8
473	Alumina films on sapphire crystal show restricted epitaxial growth. Materials Letters, 1990, 10, 75-78.	1.3	8
474	Probing the Nature and the Structure of Pores in Silica Xerogels by Water Sorption: The Tetramethyl Orthosilicate-Hydrogen Chloride/Fluoride System. Journal of the American Ceramic Society, 1991, 74, 2988-2995.	1.9	8
475	Nano- and Micro- meter Sized Silver Metal Powders by Microwave-Polyol Process. Funtai Oyobi Fummatsu Yakin/Journal of the Japan Society of Powder and Powder Metallurgy, 2003, 50, 745-750.	0.1	8
476	Topotactic Cation Exchange in Transformed Micas under Hydrothermal Conditions. Clays and Clay Minerals, 2007, 55, 593-598.	0.6	8
477	Synthesis and characterization of low-charge sodium fluorophlogopite mica-type clay minerals. Applied Clay Science, 2009, 42, 524-528.	2.6	8
478	Hydrothermal synthesis of Mn–mica. Applied Clay Science, 2009, 46, 69-72.	2.6	8
479	Microwave-Assisted Synthesis of Ag Nanophases and Their Optical Properties. Journal of Nanoscience and Nanotechnology, 2010, 10, 8035-8042.	0.9	8
480	Solvothermal synthesis of CZTS nanoparticles in ethanol: Preparation and characterization. Journal of the Korean Physical Society, 2015, 66, 1511-1515.	0.3	8
481	Synthesis of porous Al pillared montmorillonite after pre-intercalation with dodecylamine: textural and thermal properties. Journal of Porous Materials, 2016, 23, 1687-1694.	1.3	8
482	Degradation of Orange II by Fe2O3 and CeO2 nanocomposite when assisted by NaHSO3. Colloids and Surfaces A: Physicochemical and Engineering Aspects, 2021, 628, 127315.	2.3	8
483	In situ stabilization of arsenic in soil with organoclay, organozeolite, birnessite, goethite and lanthanum-doped magnetic biochar. Pedosphere, 2022, 32, 764-776.	2.1	8
484	Alternative Radwaste Solidification Route for Three Mile Island Wastes. Journal of the American Ceramic Society, 1982, 65, C-198-C-198.	1.9	7
485	Fe3+-substituted tobermorites: Synthesis and characterization by Mössbauer spectroscopy and other techniques. Materials Research Bulletin, 1985, 20, 1393-1400.	2.7	7
486	Selectivity Study of Alkaline Earth and Divalent Transition Metal lons on [Al ³⁺ + Na ⁺]-Substituted Tobermorites. Separation Science and Technology, 1993, 28, 2061-2071.	1.3	7

#	Article	IF	CITATIONS
487	Synthesis of zeolite rho: Aging temperature effect. Journal of Porous Materials, 1996, 3, 151-155.	1.3	7
488	Synthesis of swelling micas with stoichiometric amount of fluorine, characterization and ion exchange studies. Applied Clay Science, 2008, 39, 180-185.	2.6	7
489	Novel Energy-Saving Materials for Microwave Heating. Chemistry of Materials, 2008, 20, 4803-4807.	3.2	7
490	Inorganic Syntheses Assisted by Microwave Heating. Inorganics, 2015, 3, 388-391.	1.2	7
491	Facile synthesis of nanostructured porous carbon/silica composite and its adsorption property. Journal of Porous Materials, 2016, 23, 833-836.	1.3	7
492	Formation mechanism of an Al ₁₃ Keggin cluster in hydrated layered polysilicates. Dalton Transactions, 2020, 49, 4920-4926.	1.6	7
493	Composite of g-C3N4/ZnIn2S4 for efficient adsorption and visible light photocatalytic reduction of Cr(VI). Environmental Science and Pollution Research, 2022, 29, 76404-76416.	2.7	7
494	Interactions of Backfill Materials with Cesium in a Bittern Brine Under Repository Conditions. Nuclear Technology, 1982, 56, 575-579.	0.7	6
495	Immobilization of Pb2+, Cd2+, Sr2+ and Ba2+ ions using calcite and aragonite. Cement and Concrete Research, 1988, 18, 485-490.	4.6	6
496	Porosimeter as a Means to Measure the Compactibility of Powders. Journal of the American Ceramic Society, 1994, 77, 1369-1371.	1.9	6
497	Conversion of Fly Ash to Swelling Mica: A New Approach for Recycling Fly Ash. Journal of Porous Materials, 2002, 9, 291-298.	1.3	6
498	Synthesis and Characterization of Copper Hydroxide Acetate With a Layered Discoid Crystal. Journal of Materials Research, 2005, 20, 2997-3003.	1.2	6
499	Crystallization of MnO ₂ for Lithium-Ion Battery and Supercapacitor. Materials Focus, 2013, 2, 195-200.	0.4	6
500	Novel synthesis of nanophase anatase under conventional- and microwave-hydrothermal conditions: DeNOx properties. Ceramics International, 2014, 40, 2097-2102.	2.3	6
501	Formation of saponite by hydrothermal alteration of metal oxides: Implication for the rarity of hydrotalcite. American Mineralogist, 2019, 104, 1156-1164.	0.9	6
502	Degradation of methylene blue by Co ₃ O ₄ with activation of bisulfite. Functional Materials Letters, 2020, 13, 2050016.	0.7	6
503	Removal of antimonate (Sb(V)) from aqueous solutions and its immobilization in soils with a novel Fe(III)-modified montmorillonite sorbent. Environmental Science and Pollution Research, 2022, 29, 2073-2083.	2.7	6
504	Highly sensitive determination of niclosamide based on chitosan functionalized carbon nanotube/carbon black scaffolds with interconnected long- and short-range conductive network. Journal of Materials Research and Technology, 2022, 19, 4525-4535.	2.6	6

#	Article	IF	CITATIONS
505	Evaluation of SrMoO4in Repository Simulating Tests. Nuclear Technology, 1983, 62, 71-74.	0.7	5
506	Probing the pore structure and dehumidifying characteristics of chemically modified zeolite Y. Journal of Porous Materials, 1995, 1, 55-67.	1.3	5
507	Low-temperature Synthesis of Micas Under Conventional- and Microwave-Hydrothermal Conditions. Clays and Clay Minerals, 2003, 51, 693-700.	0.6	5
508	Post-isomorphic substitution of trivalent metal cations for Ca ²⁺ in portlandite crystals. RSC Advances, 2014, 4, 29305-29309.	1.7	5
509	Removal of inorganic pollutants in rainwater by a peat-derived porous material. Journal of Porous Materials, 2014, 21, 387-394.	1.3	5
510	Anthracite briquettes with plant byproducts as an ecofriendly fuel for foundries. Fuel, 2016, 175, 210-216.	3.4	5
511	Hydrothermal transformation of mixed metal oxides and silicate anions to phyllosilicate under highly alkaline conditions. Applied Clay Science, 2018, 156, 224-230.	2.6	5
512	Preparation of stable inverse emulsions of hydroxyethyl methacrylate and their stability evaluation by centrifugal coefficient. Colloids and Surfaces A: Physicochemical and Engineering Aspects, 2020, 604, 125309.	2.3	5
513	A case study targeting K fertilizer chemical synthesis with complete valorization of extraction by-products as an option. Green Chemistry, 2020, 22, 6954-6966.	4.6	5
514	Few-Layer Clayenes for Material and Environmental Applications. ACS Applied Materials & Interfaces, 2020, 12, 11171-11179.	4.0	5
515	Crystallization of MnO2 by Microwave-Hydrothermal Synthesis and Its Applications for Supercapacitors and Lithium-Ion Batteries. Materials Focus, 2013, 2, 86-91.	0.4	5
516	Optical Transmittance of AlOOH/Al2O3 Porous Gel Preforms. Journal of Sol-Gel Science and Technology, 2000, 18, 99-103.	1.1	4
517	Study on the preferred orientations of nearly cubic PZT particles synthesized by hydrothermal methods using TiCl3 reagent. Ceramics International, 2011, 37, 3211-3216.	2.3	4
518	Synthesis and Characterization of a Dual-Cation Organomontmorillonite Nanocomposite. Materials, 2018, 11, 2320.	1.3	4
519	Hydrothermal synthesis of beta zeolite from industrial silica sol as silicon source. Journal of Porous Materials, 2019, 26, 1017-1025.	1.3	4
520	Preparation of polyacrylamide–montmorillonite nanocomposite and its application in Cr(III) adsorption. Journal of Applied Polymer Science, 2020, 137, 49065.	1.3	4
521	Colloidal to micrometer-sized iron oxides and oxyhydroxides as anode materials for batteries and pseudocapacitors: Electrochemical properties. Colloids and Surfaces A: Physicochemical and Engineering Aspects, 2021, 615, 126232.	2.3	4
522	Gas-liquid-liquid extraction in a novel rotating microchannel extractor. Chinese Journal of Chemical Engineering, 2020, 28, 2523-2532.	1.7	4

#	Article	IF	CITATIONS
523	Preparation and characterization of thermal―and lightâ€triggered selfâ€healing azobenzene polymer. Polymers for Advanced Technologies, 2022, 33, 1328-1340.	1.6	4
524	Comparative study of hydrothermal stability experiments: Application to simulated nuclear waste forms. Nuclear and Chemical Waste Management, 1981, 2, 229-236.	0.2	3
525	Sandwich-Type Polymer Nanofiber Structure of Poly(furfuryl Alcohol): An Effective Template for Ordered Porous Films. Journal of Physical Chemistry B, 2009, 113, 12477-12481.	1.2	3
526	Selectivity of Co and Ni by K-depleted Micas. Clays and Clay Minerals, 2009, 57, 279-289.	0.6	3
527	Impact of Stabilizer on In Situ Formation of Ag Nanoparticles in Polyvinylidene Fluoride (PVDF) Matrix. MRS Advances, 2019, 4, 2103-2108.	0.5	3
528	Numerical simulation of the flow and erosion behavior of exhaust gas and particles in polysilicon reduction furnace. Scientific Reports, 2020, 10, 1909.	1.6	3
529	Cation Exchange and Selectivity in Heated Minerals. Soil Science Society of America Journal, 1979, 43, 790-793.	1.2	2
530	Hydrothermal synthesis of mordenite needles from erionite. Zeolites, 1986, 6, 95-98.	0.9	2
531	Phillipsite alteration in hydrothermal brines. Materials Research Bulletin, 1987, 22, 1179-1186.	2.7	2
532	Porous mullite ceramics through diphasic gels of large boehmite and small silica particles. Journal of Porous Materials, 1995, 1, 155-163.	1.3	2
533	Precipitation of hydroxyapatite film under dynamic conditions. Materials Research Bulletin, 1999, 34, 1859-1865.	2.7	2
534	Zeolitization of mineral wastes by molten-salt method: NaOH–KNO3 system. Journal of Porous Materials, 2007, 14, 37-42.	1.3	2
535	Porous solids by the pyrolysis of residue obtained after NaOH extraction of lignite. Journal of Porous Materials, 2018, 25, 897-904.	1.3	2
536	Sustainable Materials by Mimicking Natural Weathering. ACS Sustainable Chemistry and Engineering, 0,	3.2	2
537	Activation of Na ₂ S ₂ O ₈ by α-Fe ₂ O ₃ /CuS composite oxides for the degradation of Orange II under visible light irradiation. New Journal of Chemistry, 2022, 46, 4272-4282.	1.4	2
538	In situ formation of MnO2/Ni(OH)2@nickel foam with porous architecture for triggering persulfate-based advanced oxidation process. Journal of Porous Materials, 2022, 29, 1629-1637.	1.3	2
539	Nanocomposite route to the stabilization of porous ?-alumina. Journal of Porous Materials, 1995, 2, 131-134.	1.3	1
540	Preparation and thermal behavior of CaCO3/SiO2 nanocomposite. Materials Research Bulletin, 1998, 33, 1653-1660.	2.7	1

#	Article	IF	CITATIONS
541	pH dependent coprecipitated oxalate. Ferroelectrics, Letters Section, 1999, 25, 75-79.	0.4	1
542	Nanocomposite versus monophasic sol-gel processing of PLZT ceramics. Ferroelectrics, 1999, 231, 187-192.	0.3	1
543	Hydrothermal Synthesis of Ceramic Powders using Microwave Oven Funtai Oyobi Fummatsu Yakin/Journal of the Japan Society of Powder and Powder Metallurgy, 2002, 49, 884-889.	0.1	1
544	Innovations in Synthesis and Processing of Ceramic Materials. Transactions of the Indian Ceramic Society, 2004, 63, 145-149.	0.4	1
545	Porous materials: science and engineering. Materials Research Innovations, 2007, 11, 106-107.	1.0	1
546	Selective Cobalt (II) Exchange Properties of Na-2-Mica and Na-ETS-4. Solvent Extraction and Ion Exchange, 2012, 30, 524-535.	0.8	1
547	Effect of porous properties on self-cooling of fired clay plate by evaporation of absorbed water. Journal of Porous Materials, 2018, 25, 643-648.	1.3	1
548	Cleaner continuous flow production of mesoporous calcium-magnesium silicate as a potential biomaterial. Journal of Porous Materials, 2020, 27, 503-513.	1.3	1
549	Gasâ€liquidâ€liquid flow patterns and extraction in a rotating microchannel extractor. Canadian Journal of Chemical Engineering, 2021, , .	0.9	1
550	Clay coatings on sands in the western Qaidam Basin, Tibetan Plateau, China: Implications for the Martian clay detection. Applied Clay Science, 2021, 205, 106065.	2.6	1
551	Rapid Synthesis of Rod-Like Pyrolucite MnO2 by Microwave-Assisted Hydrothermal Method. Materials Focus, 2013, 2, 131-135.	0.4	1
552	Selectivity of transition metal ions by a layered tin phosphate. Materials Letters, 2022, 309, 131450.	1.3	1
553	PLZT ceramics prepared from conventional and microwave hydrothermal powders. Ferroelectrics, 1999, 231, 179-185.	0.3	Ο
554	Novel Synthetic Clays for Cation Exchange. Advances in Science and Technology, 2006, 45, 209.	0.2	0
555	Sustainable and giga-materials from plants and plant byproducts. Materials Research Innovations, 2009, 13, 413-414.	1.0	О
556	Ceramic Powders for Advanced Ceramics: What are Ideal Ceramic Powders for Advanced Ceramics?. Transactions of the Materials Research Society of Japan, 2010, 35, 473-483.	0.2	0
557	Professor Rustum Roy: In Memoriam. Materials Research Innovations, 2010, 14, 348-350.	1.0	0
558	Chemical Synthesis of LiMn2O4 and LiMn1.53Ni0.47O3.67 for Lithium-Ion Battery Anodes. Energy and Environment Focus, 2013, 2, 250-253.	0.3	0

#	Article	IF	CITATIONS
559	Rapid synthesis of α-Sn(HPO4)2·H2O by microwave-hydrothermal process. Ceramics International, 2021, 47, 16303-16308.	2.3	0
560	Preparation of lead-zirconiate-titanate using lead hydroxide by sol-gel process Journal of Advanced Science, 2000, 12, 36-37.	0.1	0
561	Microwave-Assisted Polyol Process for Synthesis of Ni Nanoparticles. Journal of the American Ceramic Society, 2006, .	1.9	0

562 Crystallization of MnO₂ for Lithium-Ion Battery and Supercapacitor (Mater. Focus Vol. 2,) Tj ETQq0 0.0 rgBT /Overlock 10

563	Solvent Effect on Photo / Thermo Responsive behaviour and Application of Poly(N-isopropylacrylamide) End-capped with 4-Propoxyazobenzene in Aqueous Media. Materials Research Innovations, 2022, 26, 44-51.	1.0	0
564	Effects of advanced oxidation on green sand properties via iron casting into green sand molds. Environmental Science & Technology, 2006, 40, 3095-101.	4.6	0